Data report: clay mineral assemblages and illite/smectite diagenesis in cuttings from Hole C0002P, IODP Expedition 348, Nankai Trough accretionary prism[1]

Michael B. Underwood[2]

Chapter contents

[1]Underwood, M.B., 2017. Data report: clay mineral assemblages and illite/smectite diagenesis in cuttings from Hole C0002P, IODP Expedition 348, Nankai Trough accretionary prism. *In* Tobin, H., Hirose, T., Saffer, D., Toczko, S., Maeda, L., Kubo, Y., and the Expedition 348 Scientists, *Proceedings of the Integrated Ocean Drilling Program,* 348: College Station, TX (Integrated Ocean Drilling Program). doi:10.2204/iodp.proc.348.204.2017
[2]Department of Earth and Environmental Science, New Mexico Institute of Mining and Technology, Socorro NM 87801, USA.
UnderwoodM@missouri.edu

Abstract

This report summarizes the results of X-ray diffraction analyses of cuttings samples (1–4 mm diameter) from Integrated Ocean Drilling Program Hole C0002P, which is located offshore southwest Japan. A total of 102 specimens (<2 µm size fraction) were analyzed from intermediate levels of the Nankai accretionary prism over a record-setting depth interval of 1975 to 3058 meters below seafloor (mbsf). Within lithologic Subunit Va, percentages of smectite in the bulk sediment average 18.0 wt% (standard deviation of 2.8), whereas values of illite and undifferentiated kaolinite + chlorite average 22.4 and 17.3 wt%, respectively (standard deviations of 3.2 and 1.8, respectively). Within lithologic Subunit Vb, percentages of smectite in the bulk sediment decrease to an average of 7.9 wt% (standard deviation of 3.4), whereas mean values of illite and kaolinite + chlorite increase to 28.4 and 22.8 wt%, respectively (standard deviations of 1.9 and 2.2, respectively). The expandability of illite/smectite mixed-layer clay within Subunit Va averages 62%, and values within Subunit Vb decrease downsection to a low of 40%. The proportion of illite in illite/smectite mixed-layer clays averages 39% within Subunit Va, and illitization within Subunit Vb increases steadily downsection to a mean of 59% illite. The illite crystallinity index shifts at approximately 2600 mbsf; values above are consistent with detrital sources that were exposed to epizone–anchizone metamorphic conditions, and values below match anchizone source conditions.

Introduction

The Nankai Trough offshore southwest Japan has been targeted by scientific ocean drilling numerous times over the past four decades (Karig, Ingle, et al., 1975; Kagami, Karig, Coulbourn, et al., 1986; Shipboard Scientific Party, 1991, 2001; Moore et al., 2005). The Nankai Trough Seismogenic Zone Experiment (NanTroSEIZE) is the latest of those efforts (Ashi et al., 2009; Screaton et al., 2009; Tobin et al., 2009; Underwood et al., 2010; Expedition 333 Scientists, 2012; Strasser et al., 2014; see the **"Expedition 348 summary"** chapter [Tobin et al., 2015a]). Integrated Ocean Drilling Program (IODP) Site C0002 is located within the NanTroSEIZE transect near the seaward edge of the Kumano Basin (Fig. **F1**). IODP Expedition 348 used riser drilling to deepen the holes at Site C0002 into the middle of the inner accretionary prism (Fig. **F2**),

doi:10.2204/iodp.proc.348.204.2017

reaching a record depth of 3058 meters below seafloor (mbsf) (see the "Expedition 348 summary" chapter [Tobin et al., 2015a]). The common lithology there is hemipelagic mudstone with variable percentages of medium siltstone to fine sandstone (turbidites). A lithologic boundary occurs at 2625 mbsf, as defined by a reduction of sandstone content and a shift from silty claystone above to fine silty claystone below (Fig. F2). Bedding planes within the accretionary prism dip at consistently steep angles.

This report summarizes the results of X-ray diffraction (XRD) analyses of 102 cuttings samples (1–4 mm) extracted from Hole C0002P. The cuttings from Hole C0002P contain nannofossils that are late Miocene (9.56–10.764 Ma) in age (see the "Site C0002" chapter [Tobin et al., 2015b]). Previous investigators of the Nankai region demonstrated that hemipelagic mud(stones) change in composition largely as function of depositional age (Cook et al., 1975; Chamley, 1980; Chamley et al., 1986; Underwood et al., 1993a, 1993b; Steurer and Underwood, 2003; Underwood and Steurer, 2003; Guo and Underwood, 2012; Underwood and Guo, 2013; Underwood and Song, 2016). As a rule, deposition of mud near the Nankai Trough during the Miocene was dominated by expandable clay minerals (smectite group), whereas proportions of detrital illite and chlorite increased steadily during the Pliocene and Quaternary. The primary objective of this report is to show whether or not samples from Hole C0002P conform to that temporal trend. A second goal is to document the diagenetic and hydration states of clay minerals (especially the smectite group). That task is important because of the clay's likely influence on fluid production within deeper levels of the accretionary prism, as well as along the landward-dipping plate interface (e.g., Saffer et al., 2008).

Methods

Sample preparation

All of the samples analyzed in this study were selected from cuttings measuring 1–4 mm in effective diameter (concentrated shipboard by wet sieving). Each extracted interval of cuttings included a companion specimen for shipboard bulk-powder XRD; those scans provided estimates of the relative abundance of total clay minerals, quartz, feldspar, and calcite (see the "Site C0002" chapter [Tobin et al., 2015b]). Isolation of clay-size fractions for XRD analyses started with air drying and gentle hand-crushing of the mudstone with mortar and pestle, after which specimens were immersed in 3% H_2O_2 for at least 24 h to digest organic matter. After adding ~250 mL of Na-hexametaphosphate solution (concentration of 4 g/1000 mL distilled H_2O), beakers were inserted into an ultrasonic bath for several minutes to promote disaggregation and deflocculation. After visual confirmation of complete disaggregation, suspensions were washed by two passes through a centrifuge (8200 revolutions per minute [rpm] for 25 min; ~6000 g) with resuspension in distilled-deionized water after each pass. The suspended sediment was then transferred to a 60 mL plastic bottle and resuspended by vigorous shaking and a 2 min application of an ultrasonic cell probe. The clay-size splits (<2 µm equivalent settling diameter) were separated by centrifugation (1000 rpm for 2.4 min; ~320 g). Preparation of oriented clay aggregates followed the filter-peel method (Moore and Reynolds, 1989b) using 0.45 µm filter membranes. A closed vapor chamber was heated to 60°C for at least 24 h to saturate the aggregates with ethylene glycol.

X-ray diffraction

The cuttings samples from Expedition 348 were analyzed at the New Mexico Bureau of Geology and Mineral Resources using a Panalytical X'Pert Pro diffractometer with Cu anode. Scans of oriented clay aggregates were run at generator settings of 45 kV and 40 mA. The continuous scans cover an angular range of 3°–26.5°2θ with a scan step time of 1.6 s, step size of 0.01°2θ, and the sample holder spinning. Slits were 1.0 mm (divergence) and 0.1 mm (receiving). MacDiff software (version 4.2.5) was used to establish a baseline of intensity, smooth counts, correct peak positions offset by misalignment of the detector (using the quartz [100] peak at 20.95°2θ; d-value = 4.24 Å), and calculate integrated peak areas (total counts). This program also calculates peak width at half height.

Calculations of mineral abundance

The most accurate analytical methods for XRD analyses require calibration with internal standards, use of single-line reference intensity ratios, and some fairly elaborate sample preparation steps to create optimal random particle orientations (e.g., Srodon et al., 2001; Omotoso et al., 2006). Given the unusually large number of samples to analyze throughout the NanTroSEIZE project, our strategy has been to obtain reliable semiquantitative accuracy with optimal efficiency. To accomplish that goal for the clay-size fraction, we recorded the integrated areas of the following peaks (Fig. F3):

- Smectite (001) centered at ~5.3°2θ (d-value = 16.5 Å);

- Illite (001) at ~8.9°2θ (d-value = 9.9 Å);
- Composite chlorite (002) + kaolinite (001) at 12.5°2θ (d-value = 7.06 Å); and
- Quartz (100) at 20.85°2θ (d-value = 4.26 Å).

Underwood et al. (2003) described the procedure for analyzing standards and computing a matrix of singular value decomposition (SVD) normalization factors (Table T1). The mixtures for those standards consist of smectite + illite + chlorite + quartz. The average errors using this method on standard mineral mixtures are 3.9% for smectite, 1.0% for illite, 1.9% for chlorite, and 1.6% for quartz. The chlorite (002) and kaolinite (001) peaks overlap almost completely, so a refined version of the Biscaye (1964) method was used to discriminate kaolinite (002) from chlorite (004), as documented by Guo and Underwood (2011). The average error of accuracy for the chlorite/kaolinite ratio is 2.6%, and that ratio was used to compute individual mineral percentages from the SVD weight percent of undifferentiated chlorite (002) + kaolinite (001). To calculate the abundance of individual clay minerals in the bulk mudstone, we multiplied each relative percentage value among the clay minerals (where smectite + illite + chlorite + kaolinite = 100%) by the percentage of total clay minerals within the bulk powder (where total clay minerals + quartz + feldspar + calcite = 100%), as determined by shipboard XRD analyses of co-located specimens (see the "Site C0002" chapter [Tobin et al., 2015b]). To facilitate direct comparisons with other published data sets from the region, this report also lists the weighted peak-area percentages for smectite, illite, and undifferentiated chlorite + kaolinite using Biscaye (1965) weighting factors (1× smectite [001], 4× illite [001], and 2× chlorite [002] + ka-olinite [001]). Errors of accuracy using that method can be substantially greater (±10% or more) than er-rors using SVD normalization factors (Underwood et al., 2003).

For documentation of clay diagenesis, the saddle/peak method of Rettke (1981) was used to calculate percent expandability of smectite and illite/smectite (I/S) mixed-layer clay (Fig. F3). This method is sensitive to the proportions of discrete illite (I) versus I/S mixed-layer clay; the curve for 1:1 mixtures of I and I/S provided the best match for the range of Nankai specimens. A complementary measure of the proportion of illite in the I/S mixed-layer phase is based on the °2θ angle of the I/S (002/003) peak (following Moore and Reynolds, 1989a), using the quartz (100) peak to correct peak positions for misalignment of the detector and/or sample holder. The I/S (002/003) peak tends to be broad and low in intensity (Fig. F3), so the center of the peak needs to be picked manually. As diagenesis advances, that peak also shifts progressively closer to the flank of the illite (002) peak, making the center peak position more difficult to judge. Values of illite crystallinity (Kübler) index are reported here as peak width at half height (Δ°2θ) for the (001) reflection.

Results

Table T2 shows the peak-area values (total counts) for common minerals in the clay-size fraction, segregated by lithologic unit. The table also includes the values of mineral abundance (wt%) calculated via SVD normalization factors and weighted peak-area percentages using Biscaye (1965) factors. Relative abundances of smectite within lithologic Subunit Va range from 39 to 21 wt%, with a mean value (μ) of 27.3 wt% and a standard deviation (σ) of 3.2. A gradual depletion of smectite with increasing depth begins at approximately 2355 mbsf (Fig. F4). Values for illite in the clay-size fraction range from 48 to 23 wt% (μ = 34.3; σ = 5.4), and those values begin to increase with depth at approximately 2355 mbsf. Percentages of kaolinite + chlorite in Subunit Va range from 32 to 20 wt% (μ = 26.4; σ = 2.9); in all cases, chlorite is the dominant mineral over kaolinite. The average percentage of clay-size quartz is 12.0 wt% (σ = 5.1). Values for clay-size smectite continue to decrease within Subunit Vb, with a range of 27–6 wt% (μ = 12.0; σ = 5.0). Abundances of illite increase steadily with depth, with a range of 45–27 wt% (μ = 43.6; σ = 3.3), whereas the content of kaolinite + chlorite ranges from 27 to 17 wt% (μ = 35.0; σ = 3.3). The average percentage of clay-size quartz is 9.4 wt% (σ = 2.2).

Figure F5 illustrates how relative mineral abundances change within the bulk sediment as a function of depth. Within lithologic Subunit Va, values of bulk sediment smectite range from 26 to 14 wt% (μ = 18.0, σ = 2.8). Those percentages are significantly lower than what Underwood and Guo (2013) documented at IODP Sites C0011 and C0012 in the Shikoku Basin (i.e., Nankai subduction inputs) (Fig. F1), where coeval (9–11 Ma) Miocene strata contain averages of 42–49 wt% smectite. Illite in the bulk sediment of Subunit Va ranges from 31 to 17 wt% (μ = 22.4, σ = 3.2), and the amount of undifferentiated kaolinite + chlorite ranges from 22 to 12 wt% (μ = 17.3, σ = 1.8). Within the bulk sediment of lithologic Subunit Vb, the abundance of smectite decreases even more to a range of 19–4 wt% (μ = 7.9, σ = 3.4). Illite in the bulk sediment ranges from 33 to 25 wt% (μ = 28.4; σ = 1.9), and kaolinite + chlorite ranges from 27 to 18 wt% (μ = 22.8; σ = 2.2).

Indicators of clay diagenesis are tabulated in Table T3 and plotted as a function of depth in Figure F6. The

expandability of I/S mixed-layer clays within Subunit Va ranges from 77% to 59%, with an average value of 62% (σ = 4.0). A steady decrease in expandability is evident with increasing depth, beginning at approximately 2350 mbsf (Fig. F6). Values within Subunit Vb range from 67% to 40% (μ = 51.0, σ = 5.8). The lowest possible value recorded by this method is 40% (i.e., saddle:peak ratio = 1.0). Within Subunit Va, the proportion of illite in I/S mixed-layer clays ranges from 16% to 53%, with an average value of 39% (σ = 10.0). Those values are scattered, with a slight increase in the proportion of illite as depth increases. Illite crystallinity (Kübler) indexes range from 0.56 to 0.23Δ°2θ, with an average value of 0.32Δ°2θ. As a frame of reference, the boundary between advanced diagenesis and anchizone metamorphism is set at 0.52Δ°2θ, and the achizone/epizone boundary (incipient greenschist facies) is 0.32Δ°2θ (Warr and Mählmann, 2015). The scatter of expandability values decreases markedly within Subunit Vb, illitization increases steadily with depth from 47% to 68% illite in the mixed-layer clay (μ = 59.0, σ = 5.5), and the average Kübler index increases to 0.42Δ°2θ. Broadening of the illite peak (i.e., lower crystallinity) seems to coincide with illitization of the I/S mixed-layer clay, as described above.

Acknowledgments

This research used samples provided by the Integrated Ocean Drilling Program (IODP). I thank the Mantle Quest Japan drilling crew, Marine Works Japan laboratory technicians, and scientists aboard D/V *Chikyu* for their dedicated assistance with sampling during IODP Expedition 348. Funding was granted by the Consortium for Ocean Leadership, U.S. Science Support Program (task order T348B58). Nolan Walla and Chen Song assisted with sample preparation. Jun Kameda provided a review of the manuscript.

References

Ashi, J., Lallemant, S., Masago, H., and the Expedition 315 Scientists, 2009. Expedition 315 summary. *In* Kinoshita, M., Tobin, H., Ashi, J., Kimura, G., Lallemant, S., Screaton, E.J., Curewitz, D., Masago, H., Moe, K.T., and the Expedition 314/315/316 Scientists, *Proceedings of the Integrated Ocean Drilling Program,* 314/315/316: Washington, DC (Integrated Ocean Drilling Program Management International, Inc.). **http://dx.doi.org/10.2204/iodp.proc.314315316.121.2009**

Biscaye, P.E., 1964. Distinction between kaolinite and chlorite in recent sediments by X-ray diffraction. *American Mineralogist,* 49:1281–1289. **http://www.minsocam.org/ammin/AM49/AM49_1281.pdf**

Biscaye, P.E., 1965. Mineralogy and sedimentation of recent deep-sea clay in the Atlantic Ocean and adjacent seas and oceans. *Geological Society of America Bulletin,* 76(7):803–831. **http://dx.doi.org/10.1130/0016-7606(1965)76[803:MASORD]2.0.CO;2**

Chamley, H., 1980. Clay sedimentation and paleoenvironment in the Shikoku Basin since the middle Miocene (Deep Sea Drilling Project Leg 58, North Philippine Sea). *In* Klein, G. de V., Kobayashi, K., et al., *Initial Reports of the Deep Sea Drilling Project,* 58: Washington, DC (U.S. Govt. Printing Office), 669–678. **http://dx.doi.org/10.2973/dsdp.proc.58.118.1980**

Chamley, H., Cadet, J.-P., and Charvet, J., 1986. Nankai Trough and Japan Trench late Cenozoic paleoenvironments deduced from clay mineralogic data. *In* Kagami, H., Karig, D.E., Coulbourn, W.T., et al., *Initial Reports of the Deep Sea Drilling Project,* 87: Washington, DC (U.S. Govt. Printing Office), 633–641. **http://dx.doi.org/10.2973/dsdp.proc.87.113.1986**

Cook, H.E., Zemmels, I., and Matti, J.C., 1975. X-ray mineralogy data, far western Pacific, Leg 31 Deep Sea Drilling Project. *In* Karig, D.E., Ingle, J.C., Jr., et al., *Initial Reports of the Deep Sea Drilling Project,* 31: Washington (U.S. Govt. Printing Office), 883–895. **http://dx.doi.org/10.2973/dsdp.proc.31.app.1975**

Expedition 333 Scientists, 2012. Expedition 333 summary. *In* Henry, P., Kanamatsu, T., Moe, K., and the Expedition 333 Scientists, *Proceedings of the Integrated Ocean Drilling Program,* 333: Tokyo (Integrated Ocean Drilling Program Management International, Inc.). **http://dx.doi.org/10.2204/iodp.proc.333.101.2012**

Guo, J., and Underwood, M.B., 2011. Data report: refined method for calculating percentages of kaolinite and chlorite from X-ray diffraction data, with application to the Nankai margin of southwest Japan. *In* Kinoshita, M., Tobin, H., Ashi, J., Kimura, G., Lallemant, S., Screaton, E.J., Curewitz, D., Masago, H., Moe, K.T., and the Expedition 314/315/316 Scientists, *Proceedings of the Integrated Ocean Drilling Program,* 314/315/316: Washington, DC (Integrated Ocean Drilling Program Management International, Inc.). **http://dx.doi.org/10.2204/iodp.proc.314315316.201.2011**

Guo, J., and Underwood, M.B., 2012. Data report: clay mineral assemblages from the Nankai Trough accretionary prism and the Kumano Basin, IODP Expeditions 315 and 316, NanTroSEIZE Stage 1. *In* Kinoshita, M., Tobin, H., Ashi, J., Kimura, G., Lallemant, S., Screaton, E.J., Curewitz, D., Masago, H., Moe, K.T., and the Expedition 314/315/316 Scientists, *Proceedings of the Integrated Ocean Drilling Program,* 314/315/316: Washington, DC (Integrated Ocean Drilling Program Management International, Inc.). **http://dx.doi.org/10.2204/iodp.proc.314315316.202.2012**

Kagami, H., Karig, D.E., Coulbourn, W.T., et al., 1986. *Initial Reports of the Deep Sea Drilling Project,* 87: Washing-

ton, DC (U.S. Govt. Printing Office). http://dx.doi.org/10.2973/dsdp.proc.87.1986

Karig, D.E., Ingle, J.C., Jr., et al., 1975. *Initial Reports of the Deep Sea Drilling Project,* 31: Washington, DC (U.S. Govt. Printing Office). http://dx.doi.org/10.2973/dsdp.proc.31.1975

Moore, D.M., and Reynolds, R.C., Jr., 1989a. Identification of mixed-layered clay minerals. *In* Moore, D.M., and Reynolds, R.C., Jr. (Eds.), *X-Ray Diffraction and the Identification and Analysis of Clay Minerals:* New York (Oxford Univ. Press USA), 241–271.

Moore, D.M., and Reynolds, R.C., Jr., 1989b. Sample preparation techniques for clay minerals. *In* Moore, D.M., and Reynolds, R.C., Jr. (Eds.), *X-Ray Diffraction and the Identification and Analysis of Clay Minerals:* New York (Oxford Univ. Press USA), 179–201.

Moore, G.F., Mikada, H., Moore, J.C., Becker, K., and Taira, A., 2005. Legs 190 and 196 synthesis: deformation and fluid flow processes in the Nankai Trough accretionary prism. *In* Mikada, H., Moore, G.F., Taira, A., Becker, K., Moore, J.C., and Klaus, A. (Eds.), *Proceedings of the Ocean Drilling Program, Scientific Results,* 190/196: College Station, TX (Ocean Drilling Program), 1–25. http://dx.doi.org/10.2973/odp.proc.sr.190196.201.2005

Omotoso, O., McCarty, D.K., Hillier, S., and Kleeberg, R., 2006. Some successful approaches to quantitative mineral analysis as revealed by the 3rd Reynolds Cup contest. *Clays and Clay Minerals,* 54(6):748–760. http://dx.doi.org/10.1346/CCMN.2006.0540609

Rettke, R.C., 1981. Probable burial diagenetic and provenance effects on Dakota Group clay mineralogy, Denver Basin. *Journal of Sedimentary Petrology,* 51(2):541–551. http://dx.doi.org/10.1306/212F7CCF-2B24-11D7-8648000102C1865D

Saffer, D.M., Underwood, M.B., and McKiernan, A.W., 2008. Evaluation of factors controlling smectite transformation and fluid production in subduction zones: application to the Nankai Trough. *Island Arc,* 17(2):208–230. http://dx.doi.org/10.1111/j.1440-1738.2008.00614.x

Screaton, E.J., Kimura, G., Curewitz, D., and the Expedition 316 Scientists, 2009. Expedition 316 summary. *In* Kinoshita, M., Tobin, H., Ashi, J., Kimura, G., Lallemant, S., Screaton, E.J., Curewitz, D., Masago, H., Moe, K.T., and the Expedition 314/315/316 Scientists, *Proceedings of the Integrated Ocean Drilling Program,* 314/315/316: Washington, DC (Integrated Ocean Drilling Program Management International, Inc.). http://dx.doi.org/10.2204/iodp.proc.314315316.131.2009

Shipboard Scientific Party, 1991. Site 808. *In* Taira, A., Hill, I., Firth, J.V., et al., *Proceedings of the Ocean Drilling Program, Initial Reports,* 131: College Station, TX (Ocean Drilling Program), 71–269. http://dx.doi.org/10.2973/odp.proc.ir.131.106.1991

Shipboard Scientific Party, 2001. Leg 190 summary. *In* Moore, G.F., Taira, A., Klaus, A., et al., *Proceedings of the Ocean Drilling Program, Initial Reports,* 190: College Station, TX (Ocean Drilling Program), 1–87. http://dx.doi.org/10.2973/odp.proc.ir.190.101.2001

Srodon, J., Drits, V.A., McCarty, D.K., Hsieh, J.C.C., and Eberl, D.D., 2001. Quantitative X-ray diffraction analysis of clay-bearing rocks from random preparations. *Clays and Clay Minerals,* 49(6):514–528. http://ccm.geoscienceworld.org/cgi/content/abstract/49/6/514

Steurer, J.F., and Underwood, M.B., 2003. Clay mineralogy of mudstones from the Nankai Trough reference Sites 1173 and 1177 and frontal accretionary prism Site 1174. *In* Mikada, H., Moore, G.F., Taira, A., Becker, K., Moore, J.C., and Klaus, A. (Eds.), *Proceedings of the Ocean Drilling Program, Scientific Results,* 190/196: College Station, TX (Ocean Drilling Program), 1–37. http://dx.doi.org/10.2973/odp.proc.sr.190196.211.2003

Strasser, M., Dugan, B., Kanagawa, K., Moore, G.F., Toczko, S., Maeda, L., Kido, Y., Moe, K.T., Sanada, Y., Esteban, L., Fabbri, O., Geersen, J., Hammerschmidt, S., Hayashi, H., Heirman, K., Hüpers, A., Jurado Rodriguez, M.J., Kameo, K., Kanamatsu, T., Kitajima, H., Masuda, H., Milliken, K., Mishra, R., Motoyama, I., Olcott, K., Oohashi, K., Pickering, K.T., Ramirez, S.G., Rashid, H., Sawyer, D., Schleicher, A., Shan, Y., Skarbek, R., Song, I., Takeshita, T., Toki, T., Tudge, J., Webb, S., Wilson, D.J., Wu, H.-Y., and Yamaguchi, A., 2014. Expedition 338 summary. *In* Strasser, M., Dugan, B., Kanagawa, K., Moore, G.F., Toczko, S., Maeda, L., and the Expedition 338 Scientists, *Proceedings of the Integrated Ocean Drilling Program,* 338: Yokohama (Integrated Ocean Drilling Program). http://dx.doi.org/10.2204/iodp.proc.338.101.2014

Tobin, H., Hirose, T., Saffer, D., Toczko, S., Maeda, L., Kubo, Y., Boston, B., Broderick, A., Brown, K., Crespo-Blanc, A., Even, E., Fuchida, S., Fukuchi, R., Hammerschmidt, S., Henry, P., Josh, M., Jurado, M.J., Kitajima, H., Kitamura, M., Maia, A., Otsubo, M., Sample, J., Schleicher, A., Sone, H., Song, C., Valdez, R., Yamamoto, Y., Yang, K., Sanada, Y., Kido, Y., and Hamada, Y., 2015a. Expedition 348 summary. *In* Tobin, H., Hirose, T., Saffer, D., Toczko, S., Maeda, L., Kubo, Y., and the Expedition 348 Scientists, *Proceedings of the Integrated Ocean Drilling Program,* 348: College Station, TX (Integrated Ocean Drilling Program). http://dx.doi.org/10.2204/iodp.proc.348.101.2015

Tobin, H., Hirose, T., Saffer, D., Toczko, S., Maeda, L., Kubo, Y., Boston, B., Broderick, A., Brown, K., Crespo-Blanc, A., Even, E., Fuchida, S., Fukuchi, R., Hammerschmidt, S., Henry, P., Josh, M., Jurado, M.J., Kitajima, H., Kitamura, M., Maia, A., Otsubo, M., Sample, J., Schleicher, A., Sone, H., Song, C., Valdez, R., Yamamoto, Y., Yang, K., Sanada, Y., Kido, Y., and Hamada, Y., 2015b. Site C0002. *In* Tobin, H., Hirose, T., Saffer, D., Toczko, S., Maeda, L., Kubo, Y., and the Expedition 348 Scientists, *Proceedings of the Integrated Ocean Drilling Program,* 348: College Station, TX (Integrated Ocean Drilling Program). http://dx.doi.org/10.2204/iodp.proc.348.103.2015

Tobin, H., Kinoshita, M., Ashi, J., Lallemant, S., Kimura, G., Screaton, E.J., Moe, K.T., Masago, H., Curewitz, D., and the Expedition 314/315/316 Scientists, 2009. NanTroSEIZE Stage 1 expeditions: introduction and synthesis of key results. *In* Kinoshita, M., Tobin, H., Ashi, J.,

Kimura, G., Lallemant, S., Screaton, E.J., Curewitz, D., Masago, H., Moe, K.T., and the Expedition 314/315/316 Scientists, *Proceedings of the Integrated Ocean Drilling Program,* 314/315/316: Washington, DC (Integrated Ocean Drilling Program Management International, Inc.). **http://dx.doi.org/10.2204/iodp.proc.314315316.101.2009**

Underwood, M.B., Basu, N., Steurer, J., and Udas, S., 2003. Data report: normalization factors for semiquantitative X-ray diffraction analysis, with application to DSDP Site 297, Shikoku Basin. *In* Mikada, H., Moore, G.F., Taira, A., Becker, K., Moore, J.C., and Klaus, A. (Eds.), *Proceedings of the Ocean Drilling Program, Scientific Results,* 190/196: College Station, TX (Ocean Drilling Program), 1–28. **http://dx.doi.org/10.2973/odp.proc.sr.190196.203.2003**

Underwood, M.B., and Guo, J., 2013. Data report: clay mineral assemblages in the Shikoku Basin, NanTroSEIZE subduction inputs, IODP Sites C0011 and C0012. *In* Saito, S., Underwood, M.B., Kubo, Y., and the Expedition 322 Scientists, *Proceedings of the Integrated Ocean Drilling Program,* 322: Tokyo (Integrated Ocean Drilling Program Management International, Inc.). **http://dx.doi.org/10.2204/iodp.proc.322.202.2013**

Underwood, M.B., Orr, R., Pickering, K., and Taira, A., 1993a. Provenance and dispersal patterns of sediments in the turbidite wedge of Nankai Trough. *In* Hill, I.A., Taira, A., Firth, J.V., et al., *Proceedings of the Ocean Drilling Program, Scientific Results*, 131: College Station, TX (Ocean Drilling Program), 15–34. **http://dx.doi.org/10.2973/odp.proc.sr.131.105.1993**

Underwood, M.B., Pickering, K., Gieskes, J.M., Kastner, M., and Orr, R., 1993b. Sediment geochemistry, clay mineralogy, and diagenesis: a synthesis of data from Leg 131, Nankai Trough. *In* Hill, I.A., Taira, A., Firth, J.V., et al., *Proceedings of the Ocean Drilling Program, Scientific Results,* 131: College Station, TX (Ocean Drilling Program), 343–363. **http://dx.doi.org/10.2973/odp.proc.sr.131.137.1993**

Underwood, M.B., Saito, S., Kubo, Y., and the Expedition 322 Scientists, 2010. Expedition 322 summary. *In* Saito, S., Underwood, M.B., Kubo, Y., and the Expedition 322 Scientists, *Proceedings of the Integrated Ocean Drilling Program,* 322: Tokyo (Integrated Ocean Drilling Program Management International, Inc.). **http://dx.doi.org/10.2204/iodp.proc.322.101.2010**

Underwood, M.B., and Song, C., 2016. Data report: clay mineral assemblages in cuttings from Hole C0002F, IODP Expedition 338, upper Nankai Trough accretionary prism. *In* Strasser, M., Dugan, B., Kanagawa, K., Moore, G.F., Toczko, S., Maeda, L., and the Expedition 338 Scientists, *Proceedings of the Integrated Ocean Drilling Program,* 338: Yokohama (Integrated Ocean Drilling Program). **http://dx.doi.org/10.2204/iodp.proc.338.206.2016**

Underwood, M.B., and Steurer, J.F., 2003. Composition and sources of clay from the trench slope and shallow accretionary prism of Nankai Trough. *In* Mikada, H., Moore, G.F., Taira, A., Becker, K., Moore, J.C., and Klaus, A. (Eds.), *Proceedings of the Ocean Drilling Program, Scientific Results,* 190/196: College Station, TX (Ocean Drilling Program), 1–28. **http://dx.doi.org/10.2973/odp.proc.sr.190196.206.2003**

Warr, L.N., and Mählmann, R.F., 2015. Recommendations for Kübler Index standardization. *Clay Minerals,* 50(3):283–286. **http://dx.doi.org/10.1180/claymin.2015.050.3.02**

Initial receipt: 10 May 2016
Acceptance: 18 November 2016
Publication: 10 March 2017
MS 348-204

Figure F1. Map of the Nankai Trough and Kumano Basin study area (NanTroSEIZE transect) with locations of Sites C0002, C0011, and C0012.

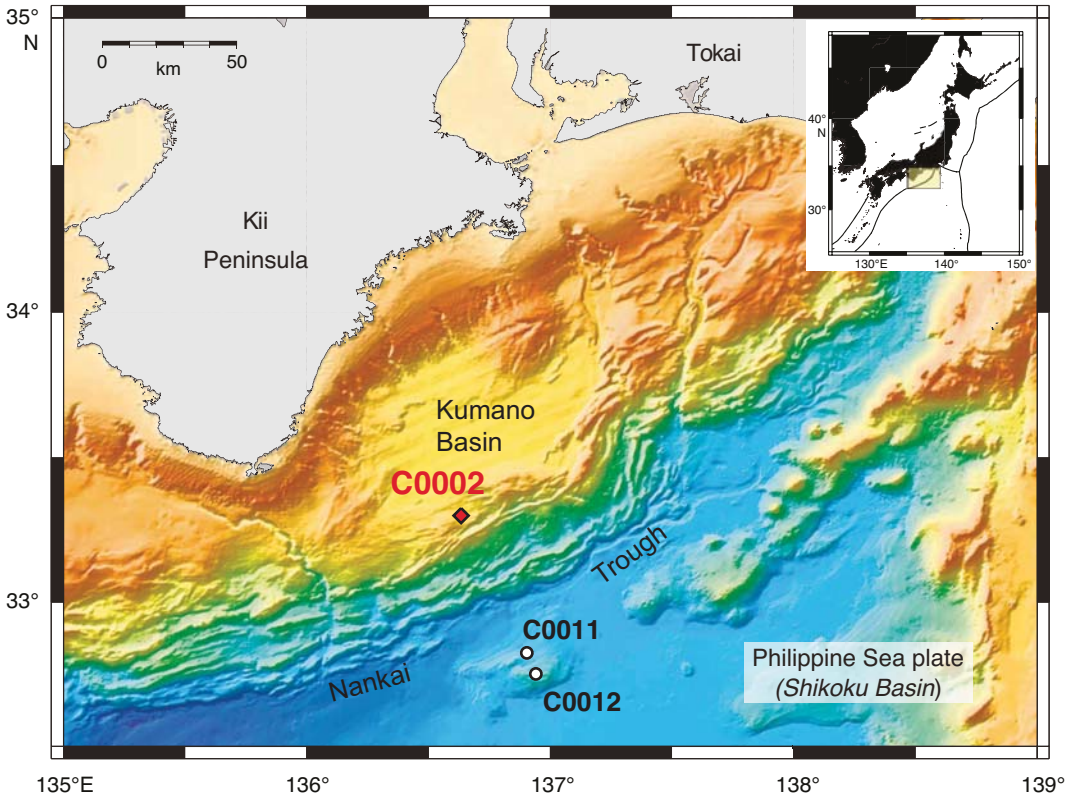

Figure F2. Seismic in-line section crossing Kumano Basin showing location of Site C0002 and lithologic units defined by shipboard analyses of cores and cuttings (see the **"Expedition 348 summary"** chapter [Tobin et al., 2015a]). LWD = logging while drilling, VE = vertical exaggeration.

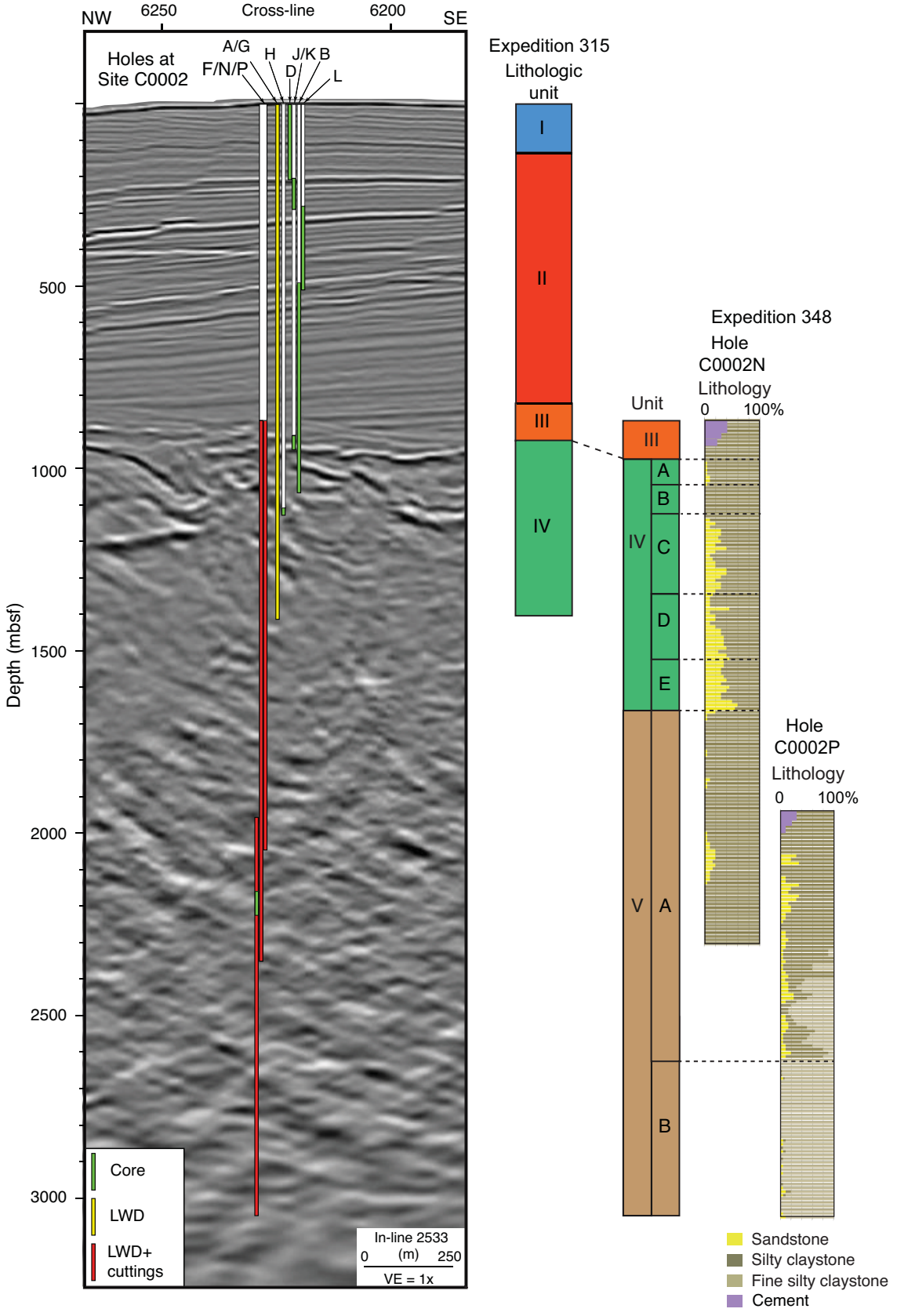

Figure F3. Representative X-ray diffractograms showing positions of peaks used to calculate relative mineral abundances and levels of clay diagenesis, Hole C0002P. S = smectite, Ch = chlorite, I = illite, K = kaolinite, I/S = illite/smectite, Q = quartz.

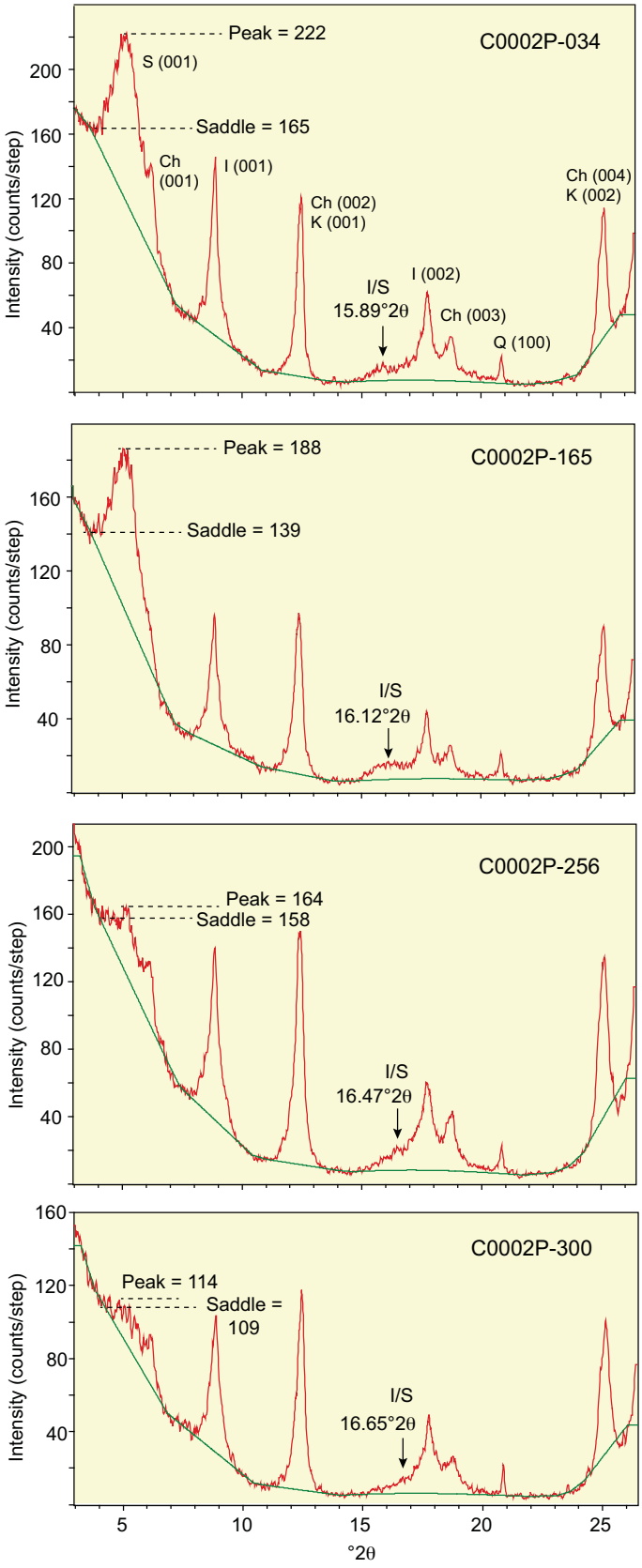

Figure F4. Calculated abundances of smectite, illite, chlorite, kaolinite, and quartz within clay-size fraction of cuttings (1–4 mm), Hole C0002P. Stratigraphic summary is from the "Expedition 348 summary" chapter (Tobin et al., 2015a).

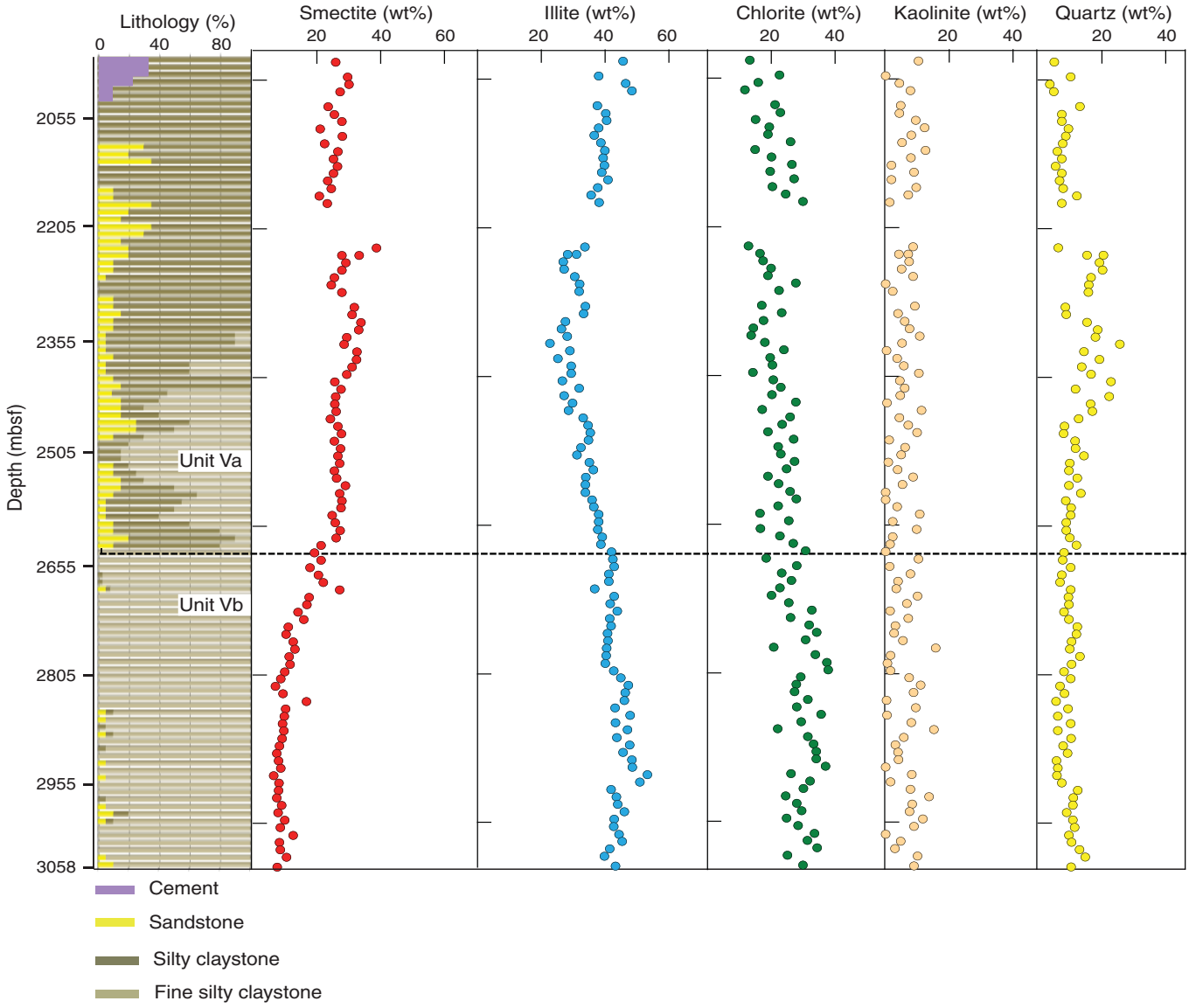

Figure F5. Calculated abundances of total clay minerals, smectite, illite, and chlorite + kaolinite within bulk sediment cuttings (1–4 mm), Hole C0002P. Values for total clay minerals are from shipboard measurements (see the "Site C0002" chapter [Tobin et al., 2015b]). Stratigraphic summary is from the "Expedition 348 summary" chapter (Tobin et al., 2015a).

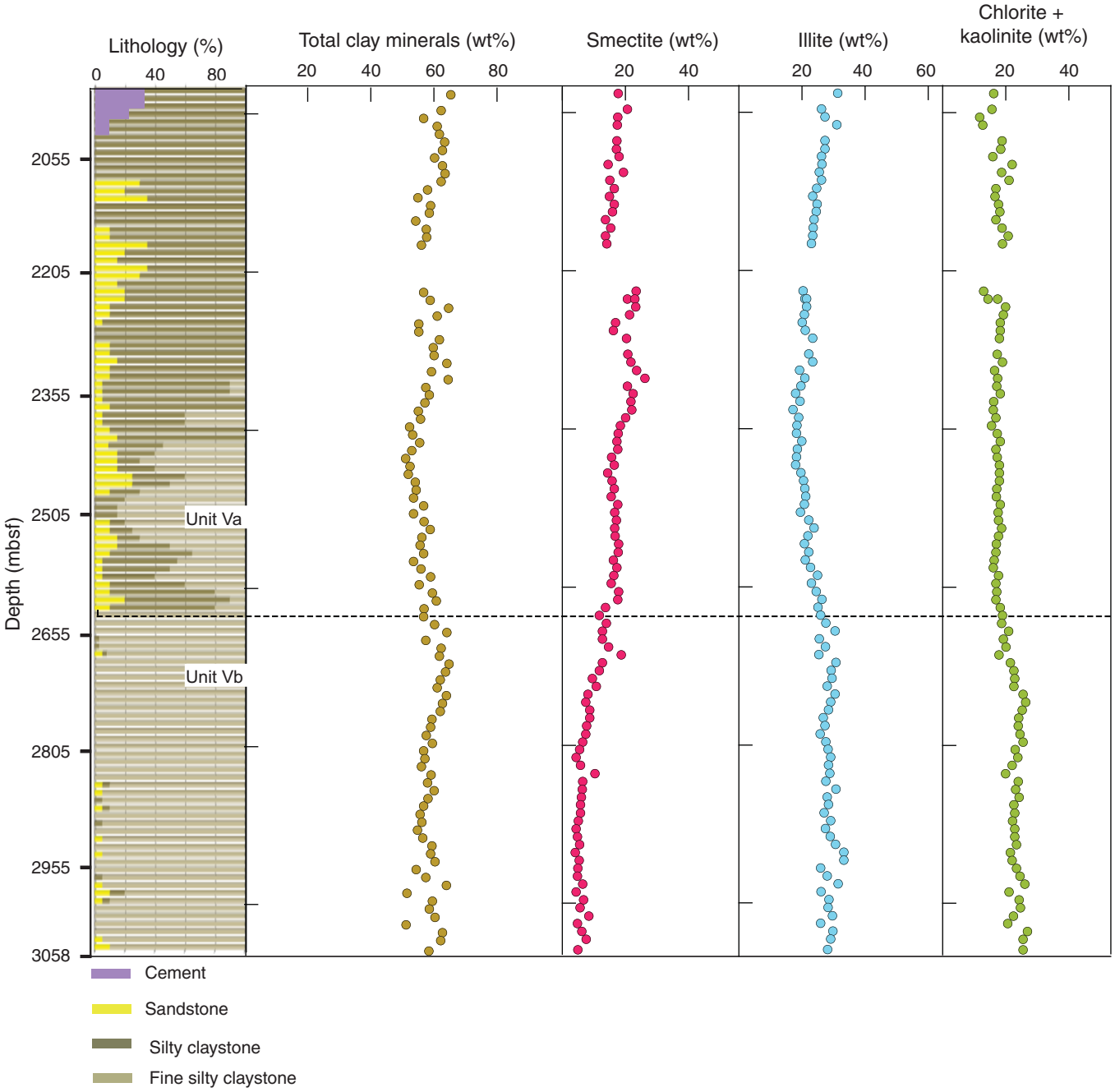

Figure F6. Illite/smectite (I/S) expandability, illite abundance in I/S mixed-layer clay, and illite crystallinity index within clay-size fraction of cuttings (1–4 mm), Hole C0002P. Boundaries for anchizone and epizone metamorphism are from Warr and Mählmann (2015). Stratigraphic summary is from the **"Expedition 348 summary"** chapter (Tobin et al., 2015a).

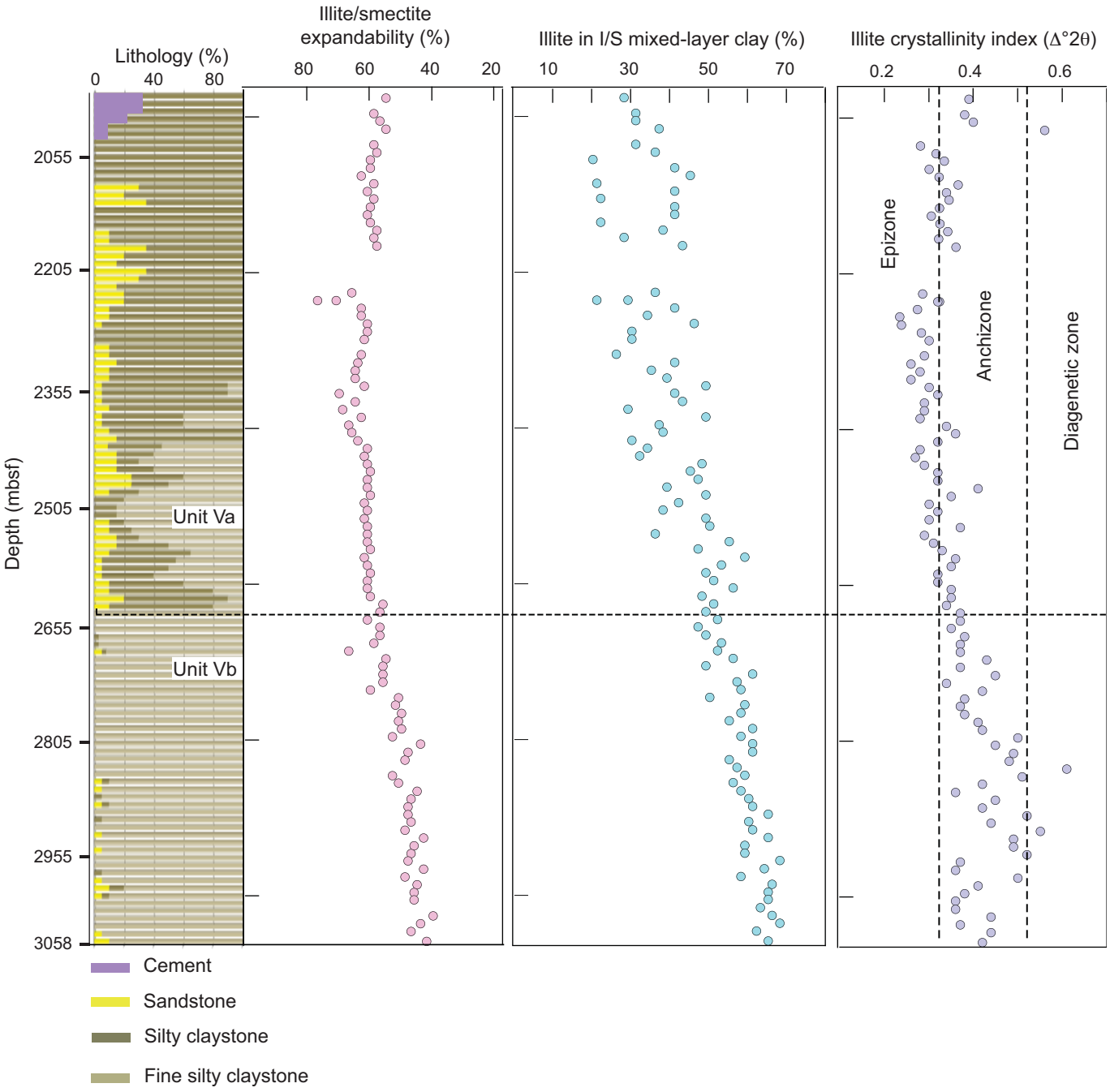

Table T1. Matrix of normalization factors used to calculate relative mineral abundances in clay-size aggregates, derived from singular value decomposition and analysis of standard mineral mixtures.

Influencing mineral	Target mineral in standard mixture			
	Smectite	Illite	Chlorite	Quartz
Smectite	7.4475294E–04	–3.1953641E–05	–7.5067212E–05	–1.5661915E–04
Illite	6.3114654E–05	3.7866938E–03	8.4222964E–05	1.1769286E–04
Chlorite	–3.5636057E–04	–6.7378140E–05	2.5121504E–03	5.2290707E–05
Quartz	9.3573136E–03	3.6491468E–03	3.2755411E–03	1.4825645E–02

Table T2. Results of X-ray diffraction analyses (<2 µm size fraction) for cuttings samples (1–4 mm), Hole C0002P. (Continued on next two pages.)

		Integrated peak area (total counts)						Relative abundance in clay-size fraction												
								SVD normalization factors (wt%)						Biscaye factors (%)			Relative abundance in bulk sediment (wt%)			
Cuttings interval number	Depth (mbsf)	Smectite (001)	Illite (001)	Composite kaolinite (001) + chlorite (002)	Quartz (100)	Composite kaolinite (002) + chlorite (004)	Half peak chlorite (004)	Smectite	Illite	Kaolinite + chlorite	Kaolinite*	Chlorite*	Quartz	Smectite	Illite	Chlorite + kaolinite	Total clay minerals	Smectite	Illite	Chlorite + kaolinite
348-C0002P-Subunit Va																				
14	1975.5	7,881	3,021	2,331	138	1,626	542	25.8	45.6	23.6	10.4	13.2	5.1	32	49	19	65.3	17.7	31.3	16.2
18	1995.5	8,983	2,717	2,393	258	1,625	819	29.6	37.9	22.5	0.0	22.5	10.1	36	44	19	62.3	20.5	26.2	15.6
20	2005.5	8,537	2,840	1,867	117	1,125	475	30.0	46.4	20.1	4.3	15.8	3.6	36	48	16	56.6	17.6	27.2	11.8
25	2015.5	7,702	3,013	1,825	129	1,036	363	27.2	48.3	19.6	7.8	11.8	4.9	33	51	16	61.0	17.4	31.0	12.6
30	2035.5	7,878	3,228	3,243	354	2,328	1,010	23.6	37.5	25.8	4.7	21.1	13.1	29	47	24	63.3	17.2	27.3	18.8
32	2045.5	10,822	3,804	3,824	250	2,729	1,207	25.4	40.2	27.2	4.4	22.8	7.3	32	45	23	62.7	17.1	27.2	18.4
34	2055.5	15,271	4,971	4,483	339	3,074	1,097	27.8	40.5	24.4	9.4	15.1	7.3	35	45	20	60.1	18.0	26.2	15.8
36	2065.5	9,730	4,024	4,962	318	3,508	1,249	21.0	38.0	31.6	12.2	19.4	9.5	27	45	28	62.7	14.5	26.3	21.9
43	2075.5	13,651	4,040	4,461	349	3,211	1,255	27.9	36.5	26.9	8.0	18.9	8.6	35	42	23	63.5	19.4	25.4	18.7
45	2085.5	10,694	4,040	4,852	274	3,523	1,551	22.4	38.7	31.2	5.2	26.0	7.7	29	44	27	62.2	15.1	26.1	21.0
47	2095.5	12,988	4,206	4,332	252	3,080	1,007	26.6	39.9	27.4	12.5	14.9	6.0	34	44	23	57.9	16.4	24.6	16.9
49	2105.5	13,045	4,506	4,782	308	3,383	1,344	25.2	39.3	28.0	7.9	20.1	7.4	32	44	24	54.9	14.9	23.3	16.6
53	2115.5	15,043	4,821	5,163	274	3,584	1,706	26.4	39.8	28.4	1.9	26.4	5.5	34	43	23	58.9	16.4	24.8	17.7
56	2125.5	13,961	4,737	5,209	322	3,558	1,369	25.2	38.9	28.7	9.0	19.7	7.3	32	44	24	58.5	15.9	24.5	18.1
58	2135.5	12,612	4,797	5,048	281	3,901	1,862	23.4	40.9	29.0	1.9	27.1	6.7	30	46	24	54.2	13.6	23.8	16.8
61	2145.5	11,801	3,999	4,770	294	3,192	1,214	24.5	37.6	30.1	9.7	20.3	7.8	32	43	26	57.6	15.3	23.5	18.8
63	2155.5	7,338	3,101	4,072	324	2,976	1,246	20.8	35.6	31.5	7.1	24.4	12.1	26	44	29	57.7	13.6	23.4	20.7
71	2165.5	9,367	3,335	4,086	228	2,905	1,409	23.2	38.1	31.3	1.3	29.9	7.4	30	43	26	56.0	14.1	23.0	18.9
107	2225.5	14,740	2,813	2,779	261	1,582	554	38.7	33.6	21.4	8.6	12.8	6.3	47	36	18	56.7	23.4	20.3	12.9
109	2235.5	6,806	2,007	2,491	484	1,744	676	27.8	28.2	23.6	7.2	16.4	20.4	34	41	25	58.8	20.5	20.9	17.4
109	2235.5	10,063	2,358	2,316	410	1,955	835	33.2	31.0	20.6	4.2	16.4	15.3	42	39	19	58.8	23.0	21.5	14.3
111	2245.5	6,677	1,674	2,353	408	1,759	687	29.1	26.9	24.8	7.4	17.4	19.2	37	37	26	64.6	23.2	21.5	19.9
113	2255.5	6,940	1,921	2,674	484	1,879	800	27.8	27.1	24.9	5.1	19.8	20.2	35	38	27	61.1	21.3	20.7	19.1
115	2265.5	6,832	2,190	2,971	382	2,098	808	25.5	30.5	27.6	8.6	19.0	16.5	32	41	28	55.2	16.8	20.1	18.2
117	2275.5	6,802	2,377	3,064	373	2,038	1,236	24.5	32.0	27.7	0.0	27.7	15.8	30	42	27	55.2	16.1	21.0	18.2
121	2285.5	8,422	2,535	2,894	411	1,962	919	27.8	31.9	24.6	2.2	22.4	15.7	35	42	24	61.7	20.3	23.4	18.0
125	2305.5	12,522	2,990	3,536	295	2,366	875	31.6	33.7	26.3	9.2	17.0	8.5	40	38	22	60.0	20.7	22.1	17.2
127	2315.5	10,579	2,540	3,143	257	2,322	1,041	31.0	33.2	27.1	3.9	23.2	8.7	39	38	23	64.0	21.7	23.3	19.0
129	2325.5	10,041	1,985	2,596	400	1,847	752	33.8	27.5	23.5	6.0	17.5	15.3	43	34	22	59.2	23.6	19.2	16.4
131	2335.5	8,986	1,839	2,327	464	1,566	582	33.1	26.3	21.9	7.6	14.3	18.6	43	35	22	64.5	26.2	20.9	17.4
133	2345.5	6,425	1,635	2,147	356	1,541	515	29.4	28.1	24.5	10.7	13.7	18.0	37	38	25	57.3	20.5	19.7	17.1
136	2355.5	5,045	1,263	2,021	522	1,352	566	28.5	22.7	23.2	5.2	18.0	25.6	36	36	29	58.5	22.4	17.9	18.2
138	2365.5	12,067	2,600	3,306	459	2,235	1,108	32.5	28.9	24.2	0.3	23.9	14.3	41	36	23	57.2	21.7	19.3	16.2
141	2375.5	3,006	599	866	163	835	370	32.4	25.1	23.5	3.7	19.7	19.1	42	34	24	55.1	22.0	17.1	16.0
143	2385.5	9,815	2,241	3,013	366	2,100	884	31.0	29.4	26.0	5.7	20.3	13.6	40	36	24	55.7	20.0	19.0	16.8

Table T2 (continued). (Continued on next page.)

		Integrated peak area (total counts)						Relative abundance in clay-size fraction: SVD normalization factors (wt%)						Relative abundance in clay-size fraction: Biscaye factors (%)			Relative abundance in bulk sediment (wt%)			
Cuttings interval number	Depth (mbsf)	Smectite (001)	Illite (001)	Composite kaolinite (001) + chlorite (002)	Quartz (100)	Composite kaolinite (002) + chlorite (004)	Half peak chlorite (004)	Smectite	Illite	Kaolinite + chlorite	Kaolinite*	Chlorite*	Quartz	Smectite	Illite	Chlorite + kaolinite	Total clay minerals	Smectite	Illite	Chlorite + kaolinite
145	2395.5	5,443	1,410	1,782	271	1,420	482	29.4	29.3	24.7	10.5	14.2	16.6	37	39	24	52.3	18.4	18.4	15.5
149	2405.5	4,661	1,565	2,225	454	1,725	752	25.6	26.5	25.0	4.5	20.5	22.9	30	41	29	53.2	17.7	18.3	17.2
151	2415.5	10,050	2,725	3,748	344	2,542	1,082	27.6	31.8	29.0	6.0	23.0	11.7	35	38	26	55.4	17.3	19.9	18.2
155	2425.5	6,426	2,151	2,946	589	2,034	882	25.8	27.1	24.8	4.6	20.2	22.3	31	41	28	53.0	17.6	18.5	16.9
157	2435.5	8,432	2,596	3,708	464	2,736	1,352	25.6	29.8	28.2	0.5	27.7	16.4	32	40	28	51.0	15.6	18.2	17.2
159	2445.5	7,379	2,148	3,252	421	2,196	771	26.0	28.5	28.4	11.3	17.1	17.0	33	38	29	52.4	16.4	18.0	17.9
161	2455.5	9,936	3,322	4,527	411	3,251	1,458	24.2	33.0	30.1	4.3	25.8	12.7	31	41	28	51.8	14.3	19.6	17.9
163	2465.5	12,948	3,710	4,918	321	3,392	1,404	26.6	34.6	30.5	7.2	23.3	8.2	34	39	26	54.1	15.7	20.4	18.0
165	2475.5	11,908	3,367	4,133	283	2,639	984	27.7	35.4	28.9	9.9	19.0	7.9	35	40	25	54.4	16.4	20.9	17.1
168	2485.5	11,395	3,723	4,481	409	3,221	1,565	25.5	34.8	28.1	1.1	27.0	11.5	32	42	25	53.5	15.4	21.1	17.0
170	2495.5	10,312	2,884	3,799	357	2,624	1,105	27.4	32.4	28.4	6.2	22.2	11.7	35	39	26	56.7	17.6	20.8	18.2
172	2505.5	10,159	3,002	4,052	455	3,191	1,393	26.5	31.2	28.0	4.9	23.0	14.3	34	40	27	53.5	16.6	19.5	17.5
174	2515.5	12,480	3,714	4,465	367	3,179	1,558	27.1	35.0	28.1	0.8	27.3	9.9	34	41	25	56.9	17.1	22.1	17.7
176	2525.5	11,579	3,813	4,467	348	3,243	1,468	25.4	36.3	28.5	3.8	24.7	9.7	32	43	25	58.8	16.6	23.7	18.6
179	2535.5	10,122	3,200	3,880	383	2,762	1,064	26.1	34.0	27.6	8.6	19.0	12.3	33	42	25	56.2	16.7	21.8	17.7
181	2545.5	12,716	3,389	4,175	353	2,848	1,227	28.9	33.8	27.6	5.3	22.3	9.7	37	39	24	55.6	17.8	20.8	17.0
183	2555.5	12,251	3,804	4,334	495	3,012	1,511	27.1	33.8	25.9	0.0	25.9	13.3	34	42	24	56.7	17.7	22.1	16.9
185	2565.5	13,355	3,874	4,517	340	3,123	1,630	27.8	35.8	27.8	0.0	27.8	8.6	35	41	24	53.5	16.2	21.0	16.3
187	2575.5	12,777	3,968	4,169	388	3,032	1,364	27.6	36.4	25.7	3.6	22.1	10.3	35	43	23	55.9	17.2	22.7	16.0
189	2585.5	10,545	3,799	4,011	339	2,924	1,031	24.8	37.9	27.1	10.7	16.4	10.2	31	45	24	58.9	16.3	24.9	17.7
191	2595.5	12,433	4,169	4,543	334	3,142	1,478	25.7	37.9	27.7	2.3	25.4	8.7	33	44	24	55.3	15.5	23.0	16.8
196	2605.5	10,803	3,397	3,547	285	2,306	834	27.3	37.6	26.3	9.8	16.5	8.8	34	43	23	59.4	17.8	24.5	17.1
198	2615.5	10,245	3,640	3,430	314	2,246	1,050	26.0	39.1	25.0	2.3	22.7	9.9	32	46	22	60.7	17.5	26.3	16.8
							Mean:	27.3	34.3	26.4	5.7	20.7	12.0				57.8	18.0	22.4	17.3
							Standard deviation:	3.2	5.4	2.9	3.5	4.5	5.1				3.6	2.8	3.2	1.8
Subunit Vb																				
200	2625.5	7,453	3,436	3,658	325	2,611	1,260	21.2	38.7	28.2	1.4	26.8	12.0	26	48	26	56.9	13.7	25.0	18.2
202	2635.5	7,738	3,788	4,081	229	2,751	1,456	19.2	42.0	30.7	0.0	30.7	8.1	25	49	26	56.6	11.8	25.9	18.9
204	2645.5	5,798	2,578	2,567	154	2,042	749	21.3	42.4	28.6	10.3	18.4	7.7	27	49	24	60.1	13.9	27.6	18.6
208	2655.5	5,823	3,410	3,390	236	2,183	1,058	17.8	42.8	29.3	1.3	28.0	10.1	22	52	26	64.0	12.7	30.5	20.9
210	2665.5	10,189	4,487	4,993	265	3,295	1,346	20.4	41.2	31.0	7.8	23.2	7.4	27	47	26	57.3	12.6	25.5	19.2
213	2675.5	11,637	4,721	5,142	272	3,344	1,520	21.9	41.1	30.2	3.9	26.3	6.9	29	46	25	62.2	14.6	27.4	20.1
215	2685.5	7,470	2,383	2,503	228	2,205	1,002	27.1	36.8	26.0	3.3	22.6	10.2	34	43	23	61.7	18.6	25.3	17.8
217	2695.5	8,445	4,851	4,961	318	3,472	1,307	17.6	42.8	30.0	10.0	20.0	9.5	22	51	26	64.8	12.6	30.7	21.5
219	2705.5	7,563	4,386	4,940	296	3,377	1,438	16.8	41.5	32.0	6.6	25.4	9.7	22	50	28	63.6	11.8	29.2	22.5
221	2715.5	6,209	4,228	4,797	217	3,018	1,467	14.0	43.8	34.1	1.4	32.7	8.1	19	52	29	61.9	9.4	29.5	22.9
224	2725.5	9,105	5,550	6,515	367	4,072	1,716	15.8	41.4	33.2	7.2	26.0	9.6	21	50	29	61.1	10.7	28.0	22.5
226	2735.5	2,961	3,142	3,794	237	2,822	1,322	11.0	41.9	34.9	3.1	31.8	12.2	13	54	33	63.9	8.0	30.5	25.4
229	2745.5	4,798	5,123	6,772	389	4,286	2,031	10.3	40.7	37.0	2.7	34.2	12.0	12	53	35	62.6	7.3	29.0	26.3
231	2755.5	5,259	4,139	5,354	286	3,310	1,478	12.5	40.8	36.2	5.4	30.7	10.5	16	51	33	62.0	8.6	28.3	25.1
233	2765.5	6,059	4,316	5,691	288	3,698	1,249	13.1	40.5	36.5	15.7	20.8	9.9	17	50	33	59.3	8.6	26.7	24.0
235	2775.5	4,256	4,412	5,625	374	3,762	1,821	11.3	40.3	35.3	1.6	33.7	13.1	13	53	34	58.9	7.7	27.3	23.9
237	2785.5	4,060	3,340	4,649	231	3,238	1,600	11.5	40.0	38.0	0.6	37.4	10.5	15	50	35	57.5	7.4	25.7	24.4
240	2795.5	3,523	3,055	4,115	146	2,847	1,383	9.9	42.7	39.4	1.6	37.8	8.0	15	51	34	59.4	6.4	27.6	25.4
242	2805.5	4,230	5,389	6,353	299	4,100	1,754	8.6	44.8	36.5	7.3	29.2	10.1	11	56	33	56.7	5.4	28.2	23.0
244	2815.5	4,683	5,775	6,863	195	4,347	1,724	7.0	47.3	38.8	11.0	27.8	6.9	11	56	33	57.2	4.3	29.1	23.8
247	2825.5	4,295	4,543	5,130	199	3,573	1,471	9.3	46.3	36.1	8.8	27.3	8.2	13	56	31	56.0	5.7	28.3	22.0
249	2835.5	3,360	1,902	1,927	73	1,277	634	16.7	46.0	31.7	0.3	31.4	5.6	23	51	26	59.1	10.4	28.8	19.9
251	2845.5	3,065	2,909	3,668	161	2,746	1,122	10.2	43.1	37.4	9.4	28.0	9.3	14	53	33	57.9	6.5	27.5	23.9
254	2855.5	5,310	4,965	5,431	162	3,412	1,690	9.8	47.9	36.1	0.5	35.6	6.2	15	55	30	60.0	6.3	30.7	23.1
256	2865.5	4,811	5,353	6,734	313	4,382	1,851	9.2	43.2	37.4	8.0	29.4	10.1	12	54	34	58.1	6.0	27.9	24.2
259	2875.5	6,640	6,076	6,989	201	4,446	1,541	9.6	47.0	37.2	15.2	22.0	6.2	15	54	31	56.7	5.8	28.4	22.5
261	2885.5	4,690	5,428	6,682	318	4,410	1,964	9.1	43.6	37.0	5.7	31.4	10.3	12	55	34	55.6	5.7	27.0	22.9

Table T2 (continued).

		Integrated peak area (total counts)						Relative abundance in clay-size fraction: SVD normalization factors (wt%)						Relative abundance in clay-size fraction: Biscaye factors (%)			Relative abundance in bulk sediment (wt%)			
Cuttings interval number	Depth (mbsf)	Smectite (001)	Illite (001)	Composite kaolinite (001) + chlorite (002)	Quartz (100)	Composite kaolinite (002) + chlorite (004)	Half peak chlorite (004)	Smectite	Illite	Kaolinite + chlorite	Kaolinite*	Chlorite*	Quartz	Smectite	Illite	Chlorite + kaolinite	Total clay minerals	Smectite	Illite	Chlorite + kaolinite
263	2895.5	4,904	5,872	6,497	229	4,162	1,955	8.2	47.6	36.4	3.1	33.3	7.8	12	57	31	56.1	5.0	29.0	22.2
265	2905.5	4,187	5,843	7,058	280	4,876	2,259	7.3	45.5	38.0	3.9	34.1	9.2	10	56	34	54.7	4.4	27.4	22.9
267	2915.5	4,415	4,731	5,405	134	3,326	1,540	7.9	48.3	38.0	4.0	34.1	5.8	13	55	32	56.4	4.7	28.9	22.8
269	2925.5	6,739	7,014	7,748	213	4,766	2,396	8.6	48.5	36.9	0.0	36.9	6.1	13	56	31	59.3	5.4	30.6	23.3
271	2935.5	5,361	7,970	7,405	194	4,799	1,984	6.5	53.2	34.4	8.2	26.2	5.9	10	61	28	58.9	4.1	33.3	21.5
273	2945.5	5,338	6,991	6,633	237	4,165	2,019	8.1	50.9	33.6	1.5	32.1	7.3	11	60	28	60.4	5.3	33.2	21.9
277	2955.5	3,107	4,952	6,482	362	4,184	1,780	7.9	41.8	37.8	7.8	30.0	12.4	9	55	36	54.3	4.9	25.9	23.4
279	2965.5	2,988	4,677	5,919	288	3,742	1,374	7.4	43.5	38.0	13.6	24.4	11.1	9	56	35	57.3	4.8	28.0	24.5
281	2975.5	3,176	4,031	4,823	245	3,201	1,331	8.9	43.9	36.4	8.4	27.9	10.8	11	56	33	63.9	6.4	31.5	26.0
283	2985.5	4,255	5,526	6,453	258	4,170	1,776	7.8	46.0	37.2	7.6	29.5	9.0	11	56	33	51.4	4.4	26.0	21.0
285	2995.5	4,505	4,991	6,163	323	3,863	1,473	9.9	42.8	36.4	11.7	24.7	10.9	12	54	33	59.4	6.6	28.5	24.3
289	3005.5	3,574	4,832	6,102	320	4,038	1,666	8.5	42.7	37.3	9.0	28.3	11.4	10	55	35	58.5	5.6	28.2	24.6
291	3015.5	2,509	2,107	2,308	121	1,984	1,002	12.5	44.4	33.5	0.0	33.5	9.6	16	54	30	60.3	8.4	29.6	22.4
293	3025.5	4,180	5,901	6,736	332	4,671	2,120	8.3	45.3	35.9	4.7	31.3	10.5	10	57	33	51.2	4.7	25.9	20.5
296	3035.5	3,258	4,982	6,482	385	4,259	2,013	8.5	41.4	37.2	2.9	34.3	12.9	9	55	36	62.7	6.1	29.8	26.8
298	3045.5	3,287	4,436	5,653	428	3,868	1,531	10.5	39.7	35.0	10.0	25.0	14.8	10	55	35	62.1	7.6	29.0	25.5
300	3058.5	2,739	3,770	4,929	217	3,334	1,387	7.5	43.2	39.0	9.0	29.9	10.3	10	54	36	58.4	4.9	28.1	25.4
							Mean:	12.0	43.6	35.0	5.8	29.2	9.4				59.0	7.9	28.4	22.8
							Standard deviation:	5.0	3.3	3.3	4.3	4.7	2.2				3.2	3.4	1.9	2.2

* = proportions of kaolinite and chlorite use ratio from Guo and Underwood (2011) method and singular value decomposition (SVD) result for undifferentiated chlorite (002) + kaolinite (001). Biscaye (1965) weighting factors are 1× smectite (001), 4× illite (001), and 2× undifferentiated chlorite (002) + kaolinite (001).

Table T3. Illite/smectite expandability values, illite abundance in illite/smectite (I/S) mixed-layer clay, and illite crystallinity index (<2 µm size fraction) for cuttings samples, Hole C0002P. (Continued on next two pages.)

Cuttings interval number	Depth (mbsf)	Smectite (001) saddle (cps)	Smectite (001) peak (cps)	Saddle:peak ratio	Expandability (%)	Illite (002) + smectite (003) (°2θ)	Illite in I/S (%)	Illite crystallinity index (Δ°2θ)
348-C0002P-Subunit Va								
14	1975.5	98	116	0.84	55	15.98	28	0.39
18	1995.5	101	132	0.77	59	16.02	31	0.38
20	2005.5	121	149	0.81	57	16.02	31	0.40
25	2015.5	109	129	0.84	55	16.10	37	0.56
30	2035.5	88	114	0.77	59	16.02	31	0.28
32	2045.5	128	163	0.79	58	16.09	36	0.32
34	2055.5	165	222	0.74	60	15.89	20	0.34
36	2065.5	133	175	0.76	60	16.16	41	0.30
43	2075.5	133	195	0.68	63	16.22	45	0.32
45	2085.5	111	143	0.78	59	15.90	21	0.37
47	2095.5	145	201	0.72	61	16.16	41	0.34
49	2105.5	150	193	0.78	59	15.91	22	0.35
53	2115.5	151	203	0.74	60	16.16	41	0.32
56	2125.5	165	223	0.74	61	16.16	41	0.31
58	2135.5	146	196	0.74	60	15.91	22	0.33
61	2145.5	144	182	0.79	58	16.11	38	0.34
63	2155.5	105	136	0.77	59	15.98	28	0.32

Table T3 (continued). (Continued on next page.)

Cuttings interval number	Depth (mbsf)	Smectite (001) saddle (cps)	Smectite (001) peak (cps)	Saddle:peak ratio	Expandability (%)	Illite (002) + smectite (003) (°2θ)	Illite in I/S (%)	Illite crystallinity index (Δ°2θ)
71	2165.5	120	152	0.79	58	16.18	43	0.36
107	2225.5	119	198	0.60	66	16.09	36	0.29
109	2235.5	27	71	0.38	77	15.99	29	0.32
109	2235.5	37	73	0.51	71	15.90	21	0.32
111	2245.5	72	105	0.69	63	16.16	41	0.27
113	2255.5	73	108	0.68	63	16.06	34	0.23
115	2265.5	84	116	0.72	61	16.23	46	0.24
117	2275.5	81	112	0.72	61	16.00	30	0.28
121	2285.5	89	127	0.70	62	16.01	30	0.30
125	2305.5	121	179	0.68	63	15.96	26	0.29
127	2315.5	107	162	0.66	64	16.15	41	0.26
129	2325.5	89	138	0.64	65	16.07	35	0.28
131	2335.5	77	119	0.65	65	16.13	39	0.26
133	2345.5	69	99	0.70	62	16.29	49	0.30
136	2355.5	41	80	0.51	70	16.15	41	0.32
138	2365.5	107	168	0.64	65	16.18	43	0.29
141	2375.5	21	39	0.54	69	15.99	29	0.29
143	2385.5	93	137	0.68	63	16.28	49	0.28
145	2395.5	44	75	0.59	67	16.10	37	0.34
149	2405.5	42	69	0.61	66	16.11	38	0.36
151	2415.5	98	148	0.66	64	16.01	30	0.32
155	2425.5	80	109	0.73	61	16.05	34	0.28
157	2435.5	96	136	0.71	62	16.03	32	0.27
159	2445.5	90	122	0.74	61	16.27	48	0.29
161	2455.5	138	183	0.75	60	16.22	45	0.32
163	2465.5	161	217	0.74	61	16.25	47	0.32
165	2475.5	139	188	0.74	61	16.12	39	0.41
168	2485.5	133	179	0.74	60	16.29	49	0.35
170	2495.5	106	152	0.70	62	16.17	42	0.30
172	2505.5	118	161	0.73	61	16.11	38	0.32
174	2515.5	148	208	0.71	62	16.28	49	0.30
176	2525.5	146	201	0.73	61	16.31	50	0.37
179	2535.5	118	163	0.72	61	16.08	36	0.29
181	2545.5	140	192	0.73	61	16.41	55	0.31
183	2555.5	135	179	0.75	60	16.26	47	0.33
185	2565.5	157	218	0.72	62	16.48	59	0.36
187	2575.5	147	199	0.74	61	16.36	53	0.35
189	2585.5	127	170	0.75	60	16.28	49	0.32
191	2595.5	146	197	0.74	61	16.33	51	0.32
196	2605.5	128	177	0.72	61	16.43	56	0.35
198	2615.5	123	165	0.75	60	16.27	48	0.35
				Mean:	62		39	0.32
				Standard deviation:	4.0		10.0	0.05
Subunit Vb								
200	2625.5	113	137	0.82	56	16.32	51	0.34
202	2635.5	132	162	0.81	57	16.29	49	0.37
204	2645.5	78	105	0.74	61	16.35	52	0.37
208	2655.5	104	129	0.81	57	16.25	47	0.35
210	2665.5	158	194	0.81	57	16.29	49	0.38
213	2675.5	158	204	0.77	59	16.37	53	0.37
215	2685.5	39	67	0.58	67	16.35	52	0.37
217	2695.5	163	194	0.84	55	16.42	56	0.43
219	2705.5	134	161	0.83	56	16.28	49	0.37
221	2715.5	131	157	0.83	56	16.53	61	0.45
224	2725.5	131	159	0.82	56	16.44	57	0.34
226	2735.5	33	44	0.75	60	16.46	58	0.42
229	2745.5	149	167	0.89	51	16.30	50	0.38
231	2755.5	129	145	0.89	52	16.50	59	0.37
233	2765.5	137	151	0.91	50	16.46	58	0.38
235	2775.5	123	138	0.89	51	16.41	55	0.41
237	2785.5	107	118	0.91	50	16.53	61	0.42
240	2795.5	79	91	0.87	53	16.46	58	0.50
242	2805.5	165	171	0.96	44	16.53	61	0.45
244	2815.5	170	182	0.93	48	16.54	61	0.49
247	2825.5	128	140	0.91	49	16.41	55	0.48
249	2835.5	*	*			16.45	57	0.61
251	2845.5	65	75	0.87	53	16.49	59	0.51
254	2855.5	135	150	0.90	51	16.43	56	0.42

Table T3 (continued).

Cuttings interval number	Depth (mbsf)	Smectite (001) saddle (cps)	Smectite (001) peak (cps)	Saddle:peak ratio	Expandability (%)	Illite (002) + smectite (003) (°2θ)	Illite in I/S (%)	Illite crystallinity index (Δ°2θ)
256	2865.5	158	164	0.96	45	16.47	58	0.36
259	2875.5	188	201	0.94	47	16.51	60	0.45
261	2885.5	162	174	0.93	48	16.54	61	0.42
263	2895.5	164	176	0.93	48	16.63	65	0.52
265	2905.5	161	171	0.94	47	16.51	60	0.44
267	2915.5	131	143	0.92	49	16.53	61	0.55
269	2925.5	230	236	0.97	43	16.64	65	0.49
271	2935.5	207	218	0.95	46	16.48	59	0.49
273	2945.5	187	199	0.94	47	16.48	59	0.52
277	2955.5	129	139	0.93	48	16.72	68	0.37
279	2965.5	133	136	0.98	43	16.61	64	0.36
281	2975.5	105	114	0.92	49	16.46	58	0.50
283	2985.5	157	164	0.96	45	16.68	66	0.41
285	2995.5	144	152	0.95	46	16.65	65	0.38
289	3005.5	141	149	0.95	46	16.65	65	0.36
291	3015.5	*	*			16.58	63	0.36
293	3025.5	173	173	1.00	40	16.68	66	0.44
296	3035.5	141	146	0.97	44	16.71	68	0.37
298	3045.5	133	142	0.94	47	16.57	62	0.44
300	3058.5	111	113	0.98	42	16.65	65	0.42
				Mean:	50.5		58.7	0.42
				Standard deviation:	5.8		5.5	0.06

* = peak intensity too low to resolve saddle/peak. cps = counts per step.